

# Conditional ablation of p63 indicates that it is essential for embryonic development of the central nervous system

Gonzalo I Cancino<sup>1</sup>, Michael P Fatt<sup>1,2</sup>, Freda D Miller<sup>1,2,3,4</sup>, and David R Kaplan<sup>1,2,4,\*</sup>

<sup>1</sup>Program in Neurosciences and Mental Health; Hospital for Sick Children; Toronto, ON Canada; <sup>2</sup>Institute of Medical Science; University of Toronto; Toronto, ON Canada;

<sup>3</sup>Departments of Physiology; University of Toronto; Toronto, ON Canada; <sup>4</sup>Molecular Genetics; University of Toronto; Toronto, ON Canada

**Keywords:** apoptosis, cortex, intermediate progenitors, neural precursor cells, neural stem cells, neurogenesis, p53, p63, p73, radial glial cells

p63 is a member of the p53 family that regulates the survival of neural precursors in the adult brain. However, the relative importance of p63 in the developing brain is still unclear, since embryonic p63<sup>-/-</sup> mice display no apparent deficits in neural development. Here, we have used a more definitive conditional knockout mouse approach to address this issue, crossing p63<sup>fl/fl</sup> mice to mice carrying a nestin-CreERT2 transgene that drives inducible recombination in neural precursors following tamoxifen treatment. Inducible ablation of p63 following tamoxifen treatment of mice on embryonic day 12 resulted in highly perturbed forebrain morphology including a thinner cortex and enlarged lateral ventricles 3 d later. While the normal cortical layers were still present following acute p63 ablation, cortical precursors and neurons were both reduced in number due to widespread cellular apoptosis. This apoptosis was cell-autonomous, since it also occurred when p63 was inducibly ablated in primary cultured cortical precursors. Finally, we demonstrate increased expression of the mRNA encoding another p53 family member, ΔNp73, in cortical precursors of p63<sup>-/-</sup> but not tamoxifen-treated p63<sup>fl/fl</sup>;R26YFP<sup>fl/fl</sup>;nestin-CreERT2<sup>+/-</sup> embryos. Since ΔNp73 promotes cell survival, then this compensatory increase likely explains the lack of an embryonic brain phenotype in p63<sup>-/-</sup> mice. Thus, p63 plays a key prosurvival role in the developing mammalian brain.

## Introduction

The p53 family consists of p53 and the closely-related proteins p63 and p73. While p53 is best-known for its role as a tumor suppressor, p63 and p73 play prominent roles during development of organisms ranging from *C. elegans* to mammals. This is best exemplified by studies of mice lacking the different family members. Mice lacking p53 are predisposed to tumors, but are largely viable,<sup>1,2</sup> although a subset of p53<sup>-/-</sup> embryos do exhibit exencephaly.<sup>3</sup> In contrast, p63<sup>-/-</sup> mice are not viable postnatally, and display profound deficits in limb and skin morphogenesis.<sup>4,5</sup> Some p73<sup>-/-</sup> mice survive to adulthood, but most die within the first few postnatal weeks, due to deficits in the immune and nervous systems.<sup>6</sup> Analyses of mice carrying floxed and isoform-specific alleles of p63 and p73 have demonstrated that at least some of these deficits are due to important roles for these 2 proteins in tissue-specific stem cell populations.<sup>7-17</sup> Thus, the highly homologous p53 family members play important but distinct roles during development.

p63 and p73 mediate their biological effects as 2 major classes of isoforms generated by alternative promoter usage. The full-length isoforms contain an N-terminal transactivation (TA) domain that is necessary for transcription, while the truncated ΔN isoforms lack the TA domain and function, at least in part, as dominant-negative proteins that inhibit their full-length counterparts either by forming inactive tetramers or by competing for promoter binding sites.<sup>18</sup> These 2 classes of isoforms are thought to play different roles in development, with the TA isoforms acting like p53 to regulate proliferation, maintain genome integrity, regulate cell metabolism and induce apoptosis, and the ΔN isoforms acting to promote cell survival and suppress senescence.<sup>18,19</sup>

Numerous studies indicate that p73 is a key protein in both the developing and adult nervous systems. The ΔNp73 isoforms are essential for survival of peripheral sympathetic and sensory neurons<sup>20-22</sup> and cortical neurons.<sup>19,23</sup> The full-length TAp73 isoforms regulate hippocampal development and self-renewal of neural stem cells, and differentiation and synaptogenesis of PNS and CNS neurons.<sup>6,24-30</sup> Analysis of mice haploinsufficient for

© Gonzalo I Cancino, Michael P Fatt, Freda D Miller, and David R Kaplan

\*Correspondence to: David R Kaplan; Email: dkaplan@sickkids.ca; Freda D Miller; Email: fredam@sickkids.ca

Submitted: 05/11/2015; Revised: 08/19/2015; Accepted: 08/22/2015

<http://dx.doi.org/10.1080/15384101.2015.1087618>

This is an Open Access article distributed under the terms of the Creative Commons Attribution-Non-Commercial License (<http://creativecommons.org/licenses/by-nc/3.0/>), which permits unrestricted non-commercial use, distribution, and reproduction in any medium, provided the original work is properly cited. The moral rights of the named author(s) have been asserted.

all isoforms of p73 have also implicated this protein in neural precursor senescence<sup>31</sup> and neurodegeneration.<sup>32-34</sup>

Like p73, p63 is an important regulator of cell survival in the postnatal nervous system, where it regulates survival of peripheral neurons.<sup>35</sup> Moreover, we recently showed that haploinsufficiency or conditional acute ablation of p63 in the adult nervous system caused the death of adult neural precursors by activation of a proapoptotic p53-PUMA pathway, thereby causing deficits in hippocampal-dependent memory formation.<sup>36</sup> However, it is still unclear whether p63 plays a role in the developing brain, since different approaches have led to different conclusions. In our own work, we showed that acute knockdown or knockout of p63 in embryonic cortical precursors using *in utero* electroporation caused precursor death via a p53-dependent pathway,<sup>37</sup> results very similar to what we reported for adult neural precursors.<sup>31,36</sup> In contrast, a second study examined the embryonic forebrain of

p63<sup>-/-</sup> mice and concluded that there were no deficits in neural development when p63 was constitutively ablated.<sup>38</sup>

Here, we have tested the hypothesis that p63 is important for embryonic brain development using a more definitive approach. Specifically, we inducibly ablated p63 in embryonic neural precursors of p63<sup>fl/fl</sup> mice with a tamoxifen-dependent nestin-CreERT2 driver line. Using this approach, we report that acute ablation of p63 leads to a robust increase in the death of neural precursors of the embryonic cortex, thereby causing cortical thinning, ventricular enlargement, and decreased numbers of embryonic cortical precursors and neurons. Moreover, we confirm, as previously published,<sup>38</sup> that there is no difference in the number of neural precursors in cortices of p63<sup>-/-</sup> and p63<sup>+/+</sup> embryos. However, we also show that  $\Delta Np73$  mRNA is specifically upregulated in p63<sup>-/-</sup> cortical precursors, suggesting that the lack of an embryonic neural phenotype in p63<sup>-/-</sup> mice is likely due to compensatory survival-

promoting mechanisms that occur within a constitutive knockout background. Thus, as we previously concluded using *in utero* electroporation,<sup>37</sup> p63 is an important prosurvival protein during embryonic neural development.

## Results

### Acute conditional deletion of p63 in embryonic neural precursors perturbs forebrain morphogenesis

To ask whether p63 plays a role during embryonic murine brain development, we crossed p63<sup>fl/fl</sup> mice to mice carrying a nestin-CreERT2 driver that efficiently promotes recombination of floxed genes in embryonic forebrain neural precursors following tamoxifen treatment.<sup>39</sup> These p63<sup>fl/fl</sup>;nestin-CreERT2<sup>+/-</sup> mice were also crossed to mice carrying a floxed YFP reporter gene in the Rosa26 locus (R26YFP<sup>fl/fl</sup>), thereby allowing us to monitor tamoxifen-induced recombination by expression of YFP. We previously used the resultant p63<sup>fl/fl</sup>;R26YFP<sup>fl/fl</sup>;nestin-CreERT2<sup>+/-</sup> mouse to inducibly ablate p63 postnatally, and showed that it was essential for the survival of adult neural precursors and adult-born neurons.<sup>36</sup> To ask about p63's developmental role, we focused on the embryonic cortex, where neurogenesis is ongoing from approximately embryonic day 12 (E12) to E18. Specifically, we treated pregnant mothers with a single intraperitoneal tamoxifen injection at E12 and analyzed coronal sections through the cortex 3 d

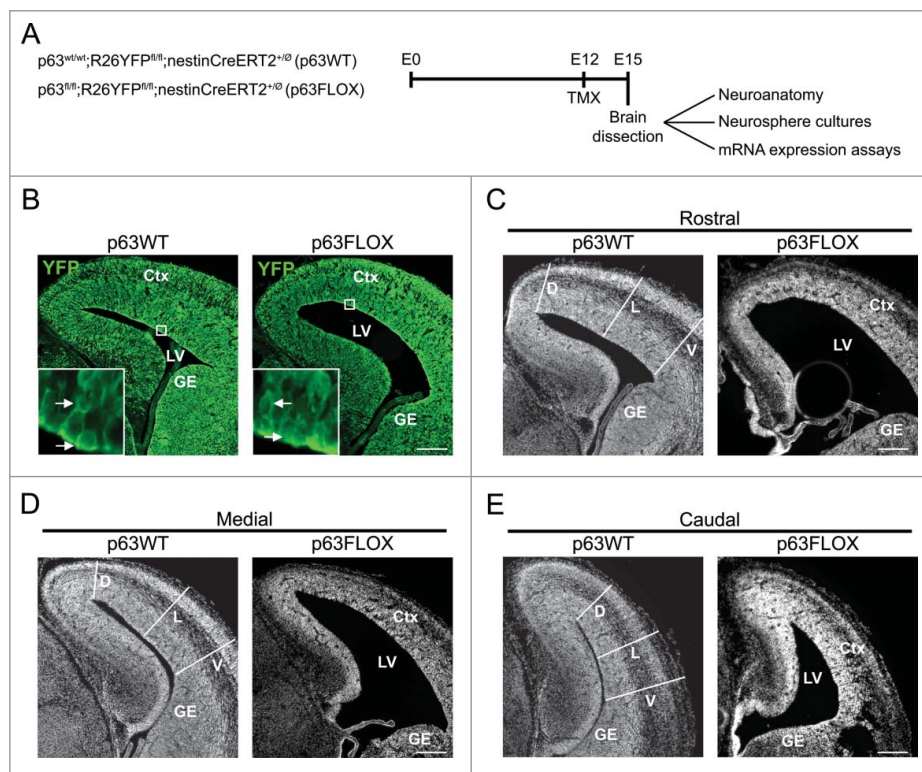


**Figure 1.** Acute inducible ablation of p63 in developing neural precursors alters embryonic forebrain morphology. **(A)** Schematic showing the experimental approach. p63<sup>wt/wt</sup>;R26YFP<sup>fl/fl</sup>;nestin-CreERT2<sup>+/-</sup> (p63WT) or p63<sup>fl/fl</sup>;R26YFP<sup>fl/fl</sup>;nestin-CreERT2<sup>+/-</sup> (p63FLOX) embryos were exposed to tamoxifen (TMX, injected into their mothers) at E12, and then their brains were analyzed 3 d later at E15. **(B)** Representative images of coronal sections through the forebrain of tamoxifen-treated p63<sup>wt/wt</sup>;R26YFP<sup>fl/fl</sup>;nestin-CreERT2<sup>+/-</sup> (p63WT, left panels) or p63<sup>fl/fl</sup>;R26YFP<sup>fl/fl</sup>;nestin-CreERT2<sup>+/-</sup> (p63FLOX, right panel) embryos immunostained for YFP to detect expression of the recombinant reporter gene. The boxed areas are shown at higher magnification in the insets, and arrows denote positive cells in the ventricular zone. The cortex (Ctx), ganglionic eminences (GE) and lateral ventricles (LV) are all denoted. Note that the YFP is present in the processes of precursors and neurons and thus the cortical layers are not easily distinguished. Scale bar = 200  $\mu$ m. **(C-E)** Representative images of coronal sections through the forebrain of p63<sup>wt/wt</sup>;R26YFP<sup>fl/fl</sup>;nestin-CreERT2<sup>+/-</sup> (p63WT, left panels) or p63<sup>fl/fl</sup>;R26YFP<sup>fl/fl</sup>;nestin-CreERT2<sup>+/-</sup> (p63FLOX, right panels) embryos at rostral **(C)**, medial **(D)**, and caudal **(E)** levels. Sections were stained with Hoechst 33258 to visualize cell nuclei. The cortex (Ctx), ganglionic eminences (GE) and lateral ventricles (LV) are all denoted. White lines illustrate where cortices were analyzed at dorsal (D), lateral (L) and ventral (V) levels. Scale bar = 200  $\mu$ m.

later, on E15 (Fig. 1A). Immunostaining for YFP showed that Cre-mediated recombination was extensive; most cells in the ventricular and subventricular precursor zones (VZ/SVZ) were

positive for YFP, as were many of the newborn neurons in the intermediate zone (IZ) and cortical plate (CP) (Fig. 1B). To ask about morphological alterations that occurred following recombination, we counterstained these sections with Hoechst 33258 to highlight nuclei. This analysis showed that the forebrain of  $p63^{fl/fl}; R26YFP^{fl/fl}; nestin-CreERT2^{+/0}$  embryos was perturbed relative to control  $p63^{wt/wt}; R26YFP^{fl/fl}; nestin-CreERT2^{+/0}$  embryos, with enlarged lateral ventricles, reduced cortical thickness and decreased ganglionic eminence size (Fig. 1C–E).

To quantify these perturbations, we focused on the cortex. Initially, we measured cortical thickness at 3 different rostral to caudal levels, making dorsal, lateral and ventral measurements at each level (Fig. 1C–E). This analysis showed that when  $p63$  was acutely ablated, cortical thickness was significantly reduced throughout the rostrocaudal extent of the cortex (Fig. 2A–C), with the largest decreases at the rostral level. We also measured the size of the lateral ventricles by determining total relative area at the same 3 rostrocaudal levels used for the cortical thickness measurements. This analysis showed that the lateral ventricles were enlarged throughout the rostrocaudal extent of the forebrain in  $p63^{fl/fl}; R26YFP^{fl/fl}; nestin-CreERT2^{+/0}$  embryos compared with control  $p63^{wt/wt}; R26YFP^{fl/fl}; nestin-CreERT2^{+/0}$  embryos (Fig. 2D). Thus, acute ablation of  $p63$  in embryonic neural precursors and their progeny from E12 to E15 was sufficient to cause cortical tissue loss and ventricular enlargement.

#### Acute conditional deletion of $p63$ induces widespread apoptosis in the embryonic forebrain

One explanation for these morphological phenotypes is that  $p63$  is essential for the survival of embryonic neural precursors and their neuronal progeny as we have shown for adult neural precursor cells.<sup>31,36</sup> To address this possibility, we assessed cell death. Initially, we isolated cortices of E15  $p63^{fl/fl}; R26YFP^{fl/fl}; nestin-CreERT2^{+/0}$  and  $p63^{wt/wt}; R26YFP^{fl/fl}; nestin-CreERT2^{+/0}$  embryos that were exposed to tamoxifen at E12, and performed qRT-PCR for  $p63$  mRNA to confirm recombination. We also analyzed *PUMA* mRNA as an indicator of enhanced p53-dependent apoptotic signaling. This analysis showed that  $p63$  mRNA levels were significantly decreased, as predicted, and that *PUMA* mRNA levels were coincidentally increased almost 2-fold (Fig. 3A). We therefore immunostained E15 cortical sections from these embryos for cleaved caspase 3 (CC3), a marker for

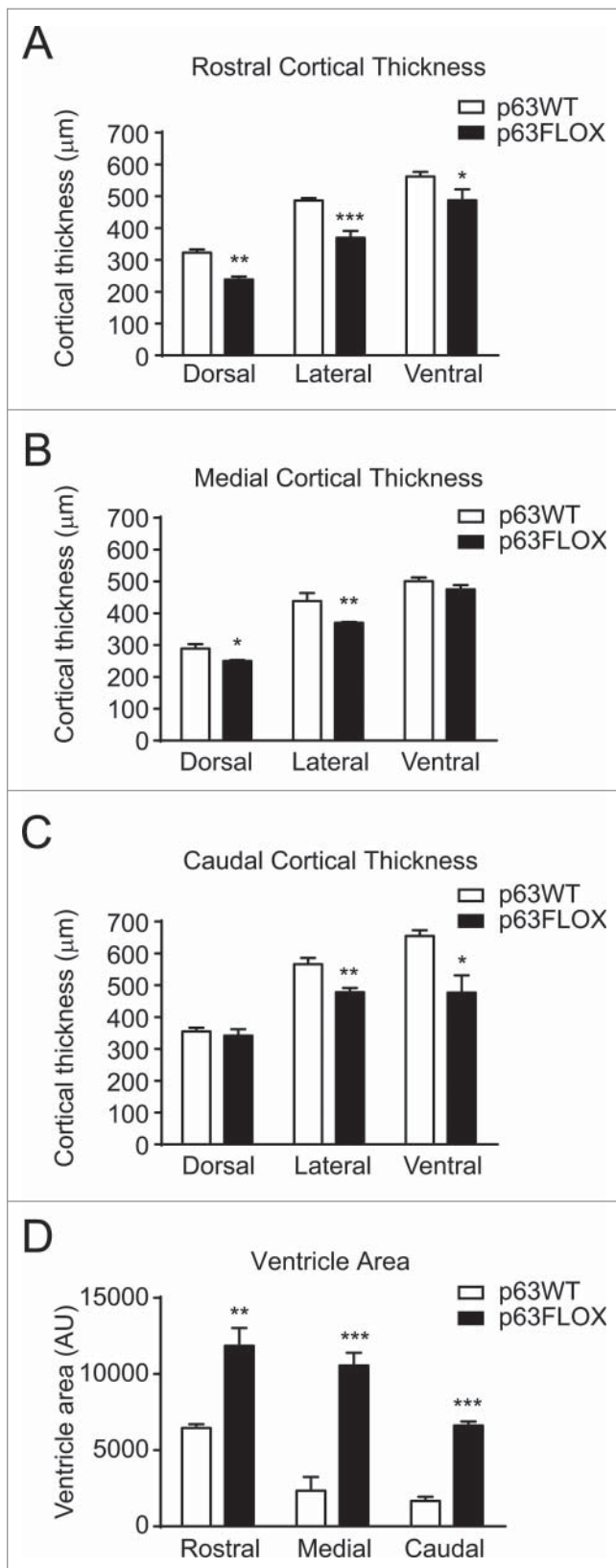


**Figure 2.** Conditional ablation of  $p63$  in cortical precursors during the neurogenic period causes reduced cortical thickness and enlarged lateral ventricles.  $p63^{wt/wt}; R26YFP^{fl/fl}; nestin-CreERT2^{+/0}$  ( $p63^{WT}$ ) or  $p63^{fl/fl}; R26YFP^{fl/fl}; nestin-CreERT2^{+/0}$  ( $p63^{FLOX}$ ) embryos were exposed to tamoxifen (injected into their mothers) at E12, and then their brains were analyzed 3 d later at E15. (A–C) Quantification of coronal forebrain sections as shown in Fig. 1 at rostral (A), medial (B), and caudal (C) levels, showing the thickness of the cortex from meninges to ventricle, as measured dorsally, laterally and ventrally. \* $p < 0.05$ ; \*\* $p < 0.01$ ; \*\*\* $p < 0.001$ ;  $n = 3$  animals per group. (D) Quantification of the relative area of the lateral ventricles in coronal forebrain sections as shown in Fig. 1 at rostral, medial and caudal levels. AU, arbitrary units; \*\* $p < 0.01$ ; \*\*\* $p < 0.001$ ;  $n = 3$  animals per group. In all panels, error bars denote SEM.

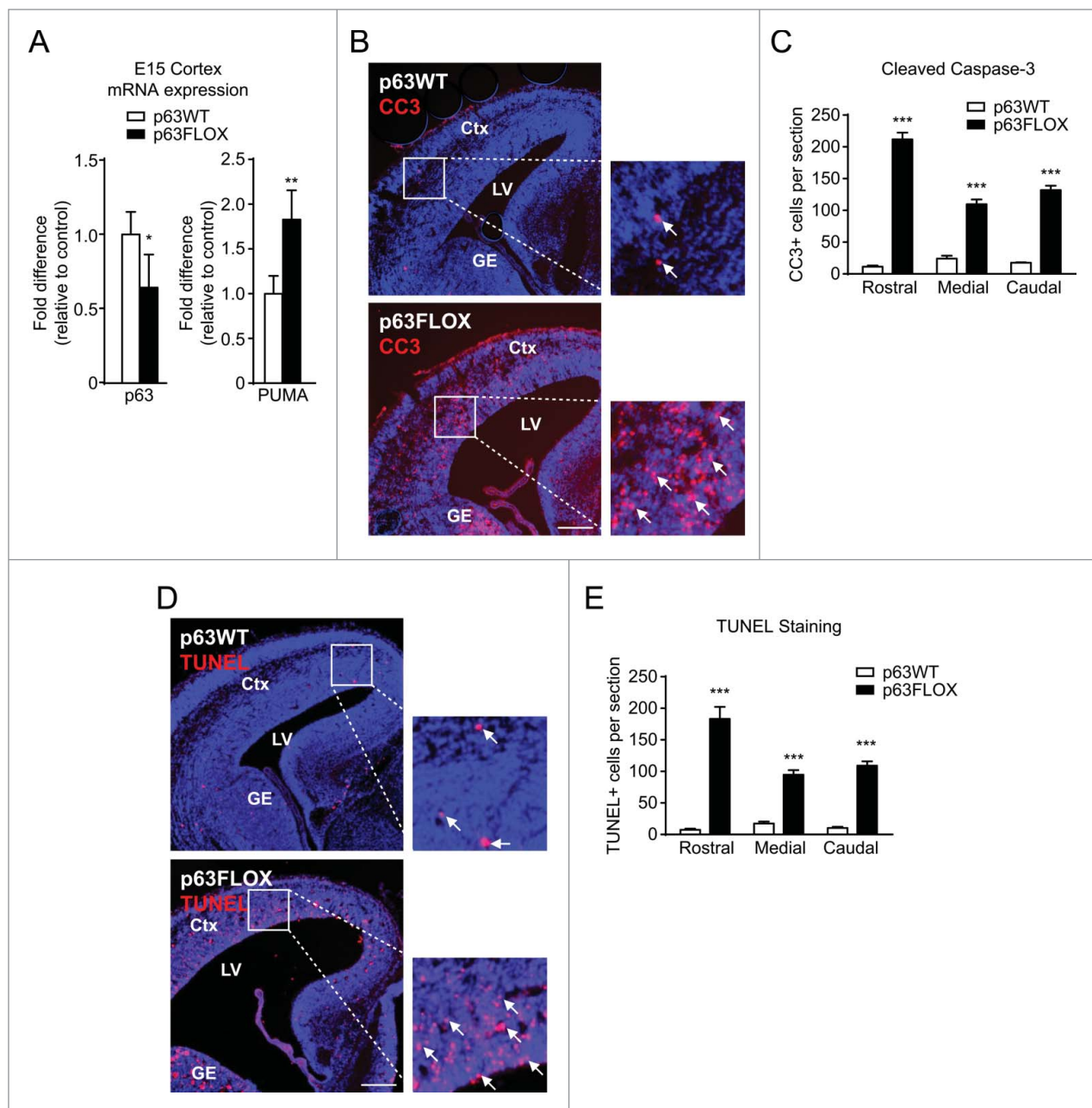


**Figure 3.** Conditional ablation of p63 in cortical precursors during the neurogenic period induces apoptosis throughout the embryonic cortex. p63<sup>wt/wt</sup>; R26YFP<sup>fl/fl</sup>; nestin-CreERT2<sup>+/-</sup> (p63WT) or p63<sup>fl/fl</sup>; R26YFP<sup>fl/fl</sup>; nestin-CreERT2<sup>+/-</sup> (p63FLOX) embryos were exposed to tamoxifen (injected into their mothers) at E12, and their cortices were analyzed 3 d later at E15. **(A)** Quantitative RT-PCR for p63 mRNA (left panel) and PUMA mRNA (right panel) comparing the relative levels of expression in p63WT and p63FLOX cortices at E15. Values are expressed as fold difference relative to the control group (p63WT). \*p < 0.05; \*\*p < 0.01; n = 4 and 5 embryos each for p63 and PUMA mRNAs respectively. **(B)** Representative images of coronal cortical sections from p63WT and p63FLOX embryos, immunostained for cleaved caspase-3 (CC3, red) and counterstained with Hoechst 33258 (blue). The boxed areas are shown at higher magnification to the right, and arrows denote CC3-positive cells. The cortex (Ctx), ganglionic eminences (GE), and lateral ventricles (LV) are all denoted. Scale bar = 200  $\mu$ m. **(C)** Quantification of sections as shown in **(B)** for the total number of CC3-positive cells in the cortex per section, determined by counting 3 similar sections per embryo at rostral, medial and caudal cortical levels. \*\*\*p < 0.001; n = 3 animals each. **(D)** Representative images of coronal cortical sections from p63WT and p63FLOX embryos, analyzed by TUNEL (red) and counterstained with Hoechst 33258 (blue). The boxed areas are shown at higher magnification to the right, and arrows denote TUNEL-positive cells. The cortex (Ctx), ganglionic eminences (GE), and lateral ventricles (LV) are all denoted. Scale bar = 200  $\mu$ m. **(E)** Quantification of sections as shown in **(D)** for the total number of TUNEL-positive cells in the cortex per section, determined by counting 3 similar sections per embryo at rostral, medial and caudal cortical levels. \*\*\*p < 0.001; n = 3 animals each. In all panels, error bars denote SEM.

apoptotic cell death. In control  $p63^{wt/wt};R26YFP^{fl/fl};nestin-CreERT2^{+/O}$  embryos, very few cortical cells were positive for CC3, as we have previously shown for wildtype cortices.<sup>37,40</sup> In contrast, large numbers of cells were CC3-positive in cortices of  $p63^{fl/fl};R26YFP^{fl/fl};nestin-CreERT2^{+/O}$  embryos treated with tamoxifen (Fig. 3B). These CC3-positive cells were scattered throughout the cortical layers, with many positive cells in the precursor zones adjacent to the lateral ventricles, and many in the upper layers of the cortex, which contain newborn neurons. There were also many CC3-positive cells in the ganglionic eminence (GE) (Fig. 3B), consistent with the decreased size of this structure (Fig. 1C–E). Quantification of cortices at rostral, medial and caudal levels showed a robust increase in CC3-positive cells, with as many as 200 cortical CC3-positive cells per section following p63 ablation (Fig. 3C).

To confirm that this large increase in CC3-positive cells following acute p63 ablation was due to enhanced apoptosis, we performed TUNEL assays for DNA fragmentation. As seen with CC3, very few TUNEL-positive cells were observed in control  $p63^{wt/wt};R26YFP^{fl/fl};nestin-CreERT2^{+/O}$  cortices following tamoxifen treatment, consistent with the low level of apoptosis in the wild-type embryonic cortex.<sup>37,40</sup> In contrast, we observed many TUNEL-positive cells in cortices of  $p63^{fl/fl};R26YFP^{fl/fl};nestin-CreERT2^{+/O}$  embryos treated with tamoxifen (Fig. 3D). As seen with CC3, these positive cells were located throughout the cortical layers, consistent with apoptosis of both precursors and newborn neurons. Quantification at rostral, medial and caudal levels indicated a highly significant increase in TUNEL-positive cells, with the magnitude similar to that seen with CC3 immunostaining (Fig. 3E). There were also many TUNEL-positive cells in the GE following p63 ablation (Fig. 3D), consistent with the CC3 data. Thus, acute ablation of p63 in neural precursors and their newborn progeny causes death of many developing forebrain cells.

#### Acute conditional deletion of p63 depletes embryonic cortical radial precursors, intermediate progenitors, and newborn neurons

To ask about the consequences of this increased apoptosis for cortical

morphogenesis, we analyzed cell type-specific markers in cortical sections from E15  $p63^{fl/fl};R26YFP^{fl/fl};nestin-CreERT2^{+/O}$  and  $p63^{wt/wt};R26YFP^{fl/fl};nestin-CreERT2^{+/O}$  embryos that were treated with tamoxifen at E12. To analyze cortical precursors, we immunostained sections for Pax6, a marker for radial precursors of the VZ/SVZ, and for Tbr2, a marker for intermediate progenitors that are found in the SVZ. This analysis (Fig. 4A) showed that both precursor populations were present and appropriately localized in the  $p63^{fl/fl};R26YFP^{fl/fl};nestin-CreERT2^{+/O}$  cortices,

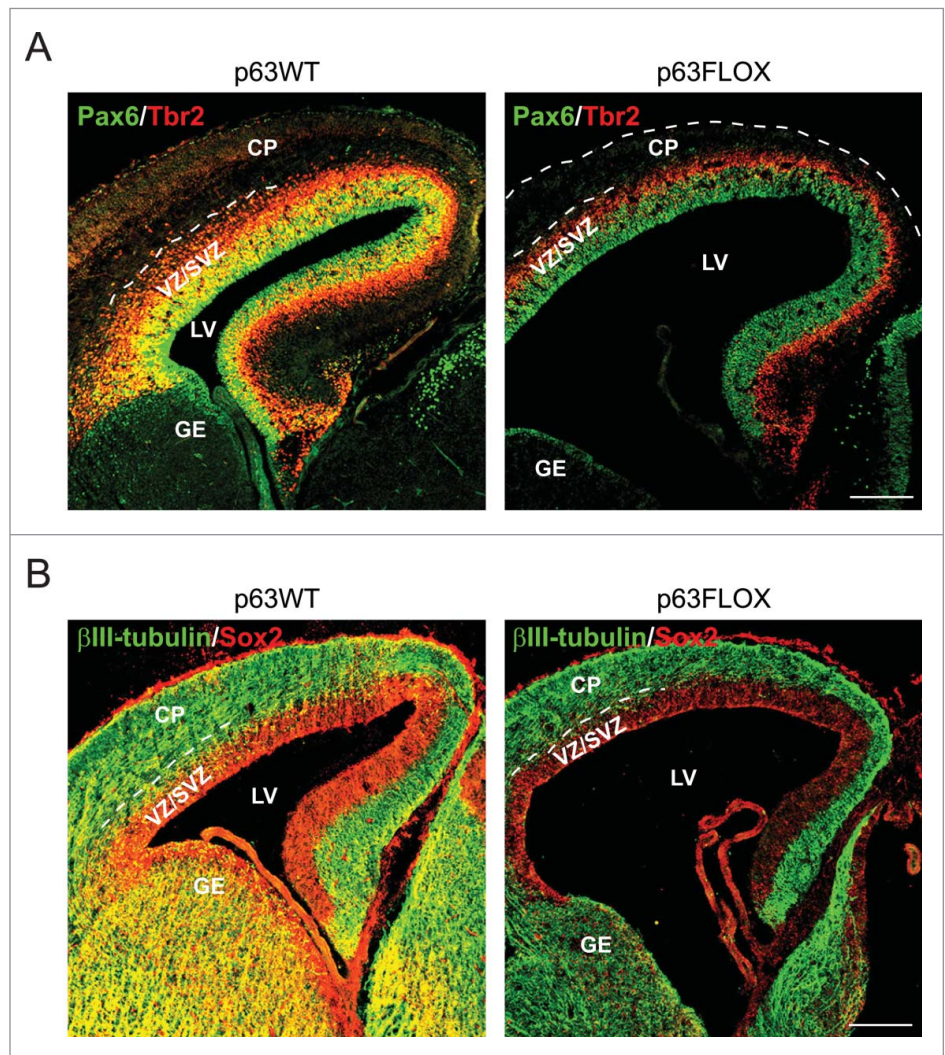


**Figure 4.** Conditional ablation of p63 in cortical precursors during the neurogenic period causes cortical thinning but not cortical disorganization.  $p63^{wt/wt};R26YFP^{fl/fl};nestin-CreERT2^{+/O}$  (p63WT) or  $p63^{fl/fl};R26YFP^{fl/fl};nestin-CreERT2^{+/O}$  (p63FLOX) embryos were exposed to tamoxifen (injected into their mothers) at E12, and their cortices were analyzed 3 d later at E15. (A) Representative images of coronal cortical sections from p63WT and p63FLOX embryos, immunostained for the radial precursor marker Pax6 (green) and the intermediate progenitor marker Tbr2 (red). The cortical plate (CP), ventricular/subventricular zones (VZ/SVZ), ganglionic eminences (GE) and lateral ventricles (LV) are all denoted. The dotted line in the right panel denotes the surface of the cortex. The boundaries of the VZ/SVZ are indicated by dotted white lines. (B) Representative images of coronal cortical sections from p63WT and p63FLOX embryos, immunostained for the neuronal marker βIII-tubulin (green) and the pan-precursor marker Sox2 (red). The cortical plate (CP), ventricular/subventricular zones (VZ/SVZ), ganglionic eminences (GE) and lateral ventricles (LV) are all denoted. The boundaries of the VZ/SVZ are indicated by dotted white lines. In all micrographs, scale bars = 200 μm.

but that the VZ/SVZ itself was thinner following acute p63 ablation. Similarly, immunostaining for the pan-precursor marker Sox2, which delineates the VZ/SVZ and the neuronal marker

$\beta$ III-tubulin, which delineates the IZ and CP (Fig. 4B) confirmed that cortical layers were appropriately organized, but that they were all relatively thinner following acute p63 ablation.

These data are consistent with the idea that cortical morphogenesis is normal following acute p63 ablation, but that the increased cell death results in decreased numbers of precursors and newborn neurons, leading to thinning of all cortical layers. To ask if this was the case, we quantified total neural precursors following immunostaining of similar sections for Sox2. To do this, we counted total marker-positive cells in a 200  $\mu$ m wide strip of the medial-lateral cortex extending from the meninges to the ventricle. This analysis demonstrated that there were less than half as many Sox2-positive precursors in p63<sup>fl/fl</sup>;R26YFP<sup>fl/fl</sup>;nestin-CreERT2<sup>+/-</sup> cortices relative to controls (Fig. 5A and B). To ask whether this was due to a reduction in radial precursors and/or intermediate progenitors, we performed a similar analysis for Pax6 (Fig. 5C and D) and Tbr2 (Fig. 5E and F). Both populations were significantly decreased by acute p63 ablation, with a larger decrease in Pax6-positive radial precursors. We performed a similar analysis for cortical neurons, immunostaining for Satb2, a marker for many of the cortical neurons that are born over the time period from E12 to E15.<sup>41</sup> This analysis demonstrated that tamoxifen treatment caused a significant decrease in Satb2-positive neurons in p63<sup>fl/fl</sup>;R26YFP<sup>fl/fl</sup>;nestin-CreERT2<sup>+/-</sup> versus control p63<sup>wt/wt</sup>;R26YFP<sup>fl/fl</sup>;nestin-CreERT2<sup>+/-</sup> cortices (Fig. 5G and H), confirming the reduction in cortical neurons suggested by the decrease in  $\beta$ III-tubulin immunostaining (Fig. 4B).

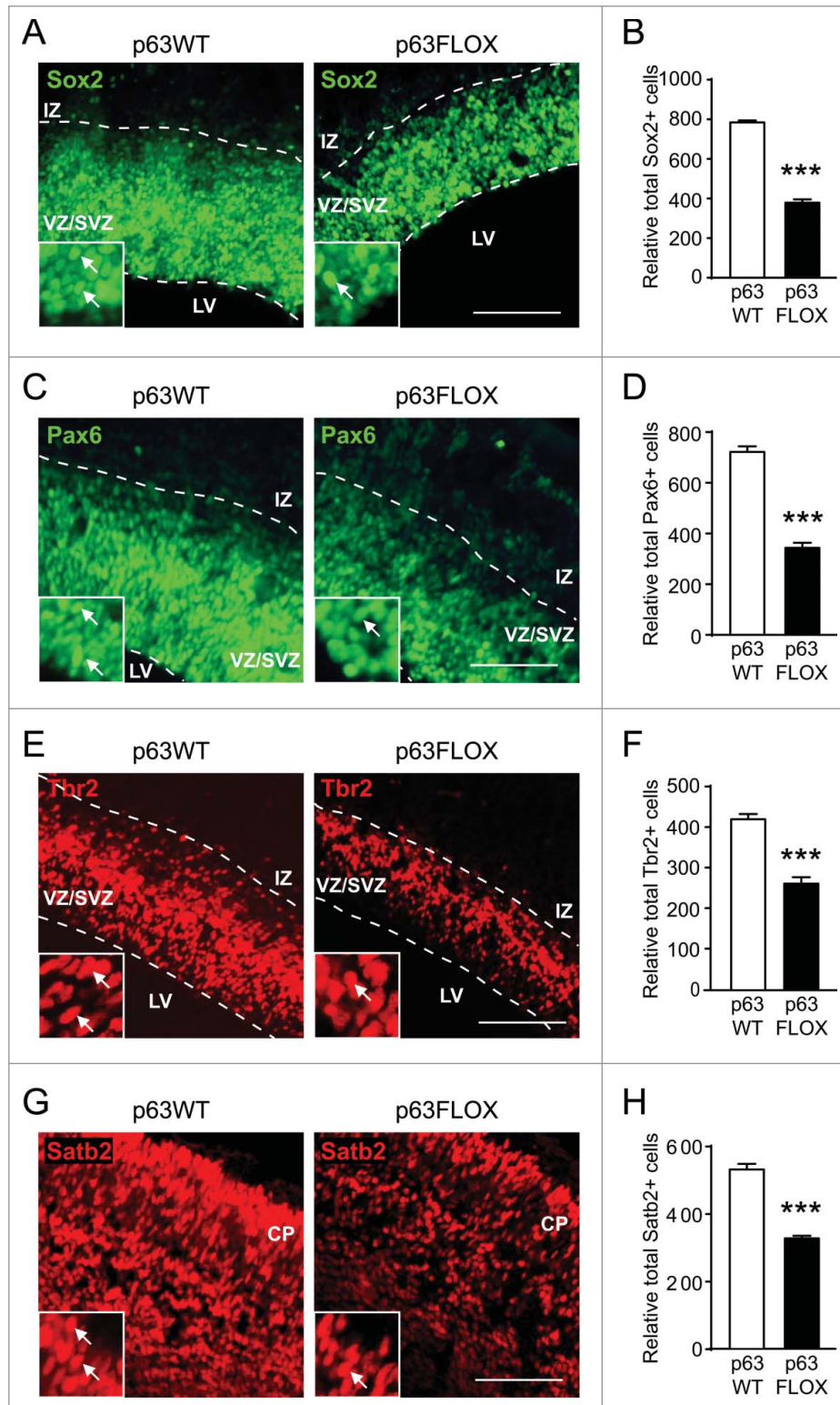


**Figure 5.** For figure legend, see page 3276.

#### Embryonic cortical precursors display a cell-autonomous deficit in cell survival following acute p63 ablation

To further confirm that acute ablation of p63 in neural precursors causes enhanced cell death, we turned to cell culture experiments. Initially, we treated p63<sup>fl/fl</sup>;R26YFP<sup>fl/fl</sup>;nestin-CreERT2<sup>+/-</sup> vs. control p63<sup>wt/wt</sup>;R26YFP<sup>fl/fl</sup>;nestin-CreERT2<sup>+/-</sup> embryos with tamoxifen at E12 and then isolated neurospheres from the embryonic cortices. Quantification of the number of primary

neurosphere-initiating cells, a surrogate measure of neural precursor numbers, demonstrated that they were decreased more than 2-fold following acute p63 ablation *in vivo* (Fig. 6A). qRT-PCR analysis of the RNA from these neurospheres confirmed that p63 mRNA was highly reduced, but that expression of the other family members was unaltered (Fig. 6B).

To further establish a role for p63 in cortical precursor survival, we performed inducible ablation experiments in primary adherent cultures of developing cortical radial precursors. Specifically, we cultured p63<sup>fl/fl</sup>;R26YFP<sup>fl/fl</sup>;nestin-CreERT2<sup>+/-</sup> versus control p63<sup>wt/wt</sup>; R26YFP<sup>fl/fl</sup>;nestin-CreERT2<sup>+/-</sup> cortical precursors from E12.5 mice, and after 2 d added increasing concentrations of tamoxifen to induce ablation of p63 and expression of YFP. We immunostained these cultures one day later for CC3 and YFP (Fig. 6C). Quantification demonstrated a robust increase in apoptosis of YFP-positive precursors that was dependent upon the dose of tamoxifen (Fig. 6D).

### $\Delta Np73$ mRNA is increased in cortical precursors when p63 is constitutively knocked-out

These data provide strong support for the idea that p63 is required in a cell-autonomous fashion to support the survival of cortical precursors and newborn neurons both in culture and *in vivo*. However, a previous study examined the cortices of embryonic p63<sup>-/-</sup> mice and concluded that p63 was not necessary for the survival of either precursors or neurons.<sup>38</sup> One explanation for this discrepancy is that in the constitutive knockout situation, other family members compensate for the loss of p63.<sup>42</sup> To test this idea, we cultured E15 cortical precursors from p63<sup>+/-</sup> vs. p63<sup>-/-</sup> mice as neurospheres. As previously reported,<sup>38</sup> and in contrast to the robust decrease in cortical neurosphere-initiating cells in tamoxifen treated p63<sup>fl/fl</sup>;R26YFP<sup>fl/fl</sup>;nestin-CreERT2<sup>+/-</sup> embryos (Fig. 6A), there was no difference in the number of neurosphere-initiating cells cultured from p63<sup>-/-</sup> versus p63<sup>+/-</sup> cortices (Fig. 6E). However, while qRT-PCR analysis showed that the levels of *TAp73* and *p53* mRNA were unaltered in

p63<sup>-/-</sup> neurospheres, the levels of  $\Delta Np73$  mRNA, a pro-survival member of the p53 family, were upregulated by 2-fold (Fig. 6F).

To ask if this compensatory increase in  $\Delta Np73$  mRNA also occurred *in vivo*, we crossed p63<sup>+/-</sup> mice, and then analyzed cortical precursors in their p63<sup>+/-</sup> vs. p63<sup>-/-</sup> embryonic progeny. To do so, we analyzed E15 coronal cortical sections by immunostaining for Sox2 to identify cortical precursor cells, combined with *in situ* hybridization with a probe specific for  $\Delta Np73$  mRNA (Fig. 6G). Quantification of this data demonstrated that while similar numbers of Sox2-positive cortical precursors expressed  $\Delta Np73$  mRNA in p63<sup>-/-</sup> versus p63<sup>+/-</sup> embryos, approximately 64% and 59%, respectively,  $\Delta Np73$  mRNA levels were increased in the p63<sup>-/-</sup> cortical precursors, 3.7 vs. 2.0  $\Delta Np73$  mRNA grains per Sox2-positive cell in p63<sup>-/-</sup> versus p63<sup>+/-</sup> cortices, respectively. Since  $\Delta Np73$  is a key prosurvival protein in the embryonic cortex,<sup>19,23,37,43-45</sup> then this compensatory increase likely provides an explanation for the lack of an apoptotic phenotype in the p63<sup>-/-</sup> embryonic cortex as shown by Holembowski et al.<sup>38</sup>

## Discussion

The work presented here definitively establishes that p63 plays an important prosurvival role in the embryonic central nervous system (CNS). Inducible ablation of p63 in embryonic neural precursors and their newborn neuronal progeny led to a robust increase in apoptosis of forebrain precursors and neurons, and perturbed cortical morphogenesis. The overall organization of the cortical layers was unchanged, but there were many fewer radial precursors, neurogenic intermediate progenitors and neurons, decreases that caused thinning of the cortex and enlargement of the ventricles. This cell death phenotype was cell autonomous, since inducible ablation of p63 in cultured precursors also caused apoptosis. These findings are very similar to those obtained using *in utero* electroporation to knockdown p63 in the embryonic cortex,<sup>37</sup> but are different from those obtained by

**Figure 5 (See previous page).** Cortical precursors and newborn neurons are reduced in number following conditional ablation of p63. p63<sup>wt/wt</sup>; R26YFP<sup>fl/fl</sup>;nestin-CreERT2<sup>+/-</sup> (p63WT) or p63<sup>fl/fl</sup>;R26YFP<sup>fl/fl</sup>;nestin-CreERT2<sup>+/-</sup> (p63FLOX) embryos were exposed to tamoxifen (injected into their mothers) at E12, and their cortices were analyzed 3 d later at E15. **(A)** Representative images of the VZ/SVZ of coronal cortical sections from p63WT and p63FLOX embryos, immunostained for Sox2 (green; the endogenous YFP is not seen under these excitation/emission conditions). Insets show higher magnification images and the arrows denote Sox2-positive cells. The boundaries of the VZ/SVZ are indicated by dotted white lines. Scale bar = 100  $\mu$ m. **(B)** Quantification of the total number of Sox2-positive cells in a strip of the lateral-medial cortex extending from the meninges to the ventricle, determined from sections as in **(A)**. \*\*\*p < 0.001; n = 3 sections per embryo and 3 embryos per genotype (9 sections total). **(C)** Representative images of the VZ/SVZ of coronal cortical sections from p63WT and p63FLOX embryos, immunostained for Pax6 (green; the endogenous YFP is not seen under these excitation/emission conditions). Insets show higher magnification images and the arrows denote Pax6-positive cells. The boundaries of the VZ/SVZ are indicated by dotted white lines. Scale bar = 100  $\mu$ m. **(D)** Quantification of the total number of Pax6-positive cells in a strip of the medial-lateral cortex extending from the meninges to the ventricle, determined from sections as in **(C)**. \*\*\*p < 0.001; n = 3 sections per embryo and 3 embryos per genotype (9 sections total). **(E)** Representative images of the VZ/SVZ of coronal cortical sections from p63WT and p63FLOX embryos, immunostained for Tbr2 (red). Insets show higher magnification images and the arrows denote Tbr2-positive cells. The boundaries of the VZ/SVZ are indicated by dotted white lines. Scale bar = 100  $\mu$ m. **(F)** Quantification of the total number of Tbr2-positive cells in a strip of the medial-lateral cortex extending from the meninges to the ventricle, determined from sections as in **(E)**. \*\*\*p < 0.001; n = 3 sections per embryo and 3 embryos per genotype (9 sections total). **(G)** Representative images of the cortical plate of coronal cortical sections from p63WT and p63FLOX embryos, immunostained for Satb2 (red). Insets show higher magnification images and the arrows denote Satb2-positive cells. Scale bar = 100  $\mu$ m. **(H)** Quantification of the total number of Satb2-positive cells in a strip of the medial-lateral cortex extending from the meninges to the ventricle, determined from sections as in **(G)**. \*\*\*p < 0.001; n = 3 sections per embryo and 3 embryos per genotype (9 sections total). The cortical plate (CP), ventricular/subventricular zones (VZ/SVZ), intermediate zone (IZ) and lateral ventricles (LV) are all denoted. In all panels, error bars denote SEM.

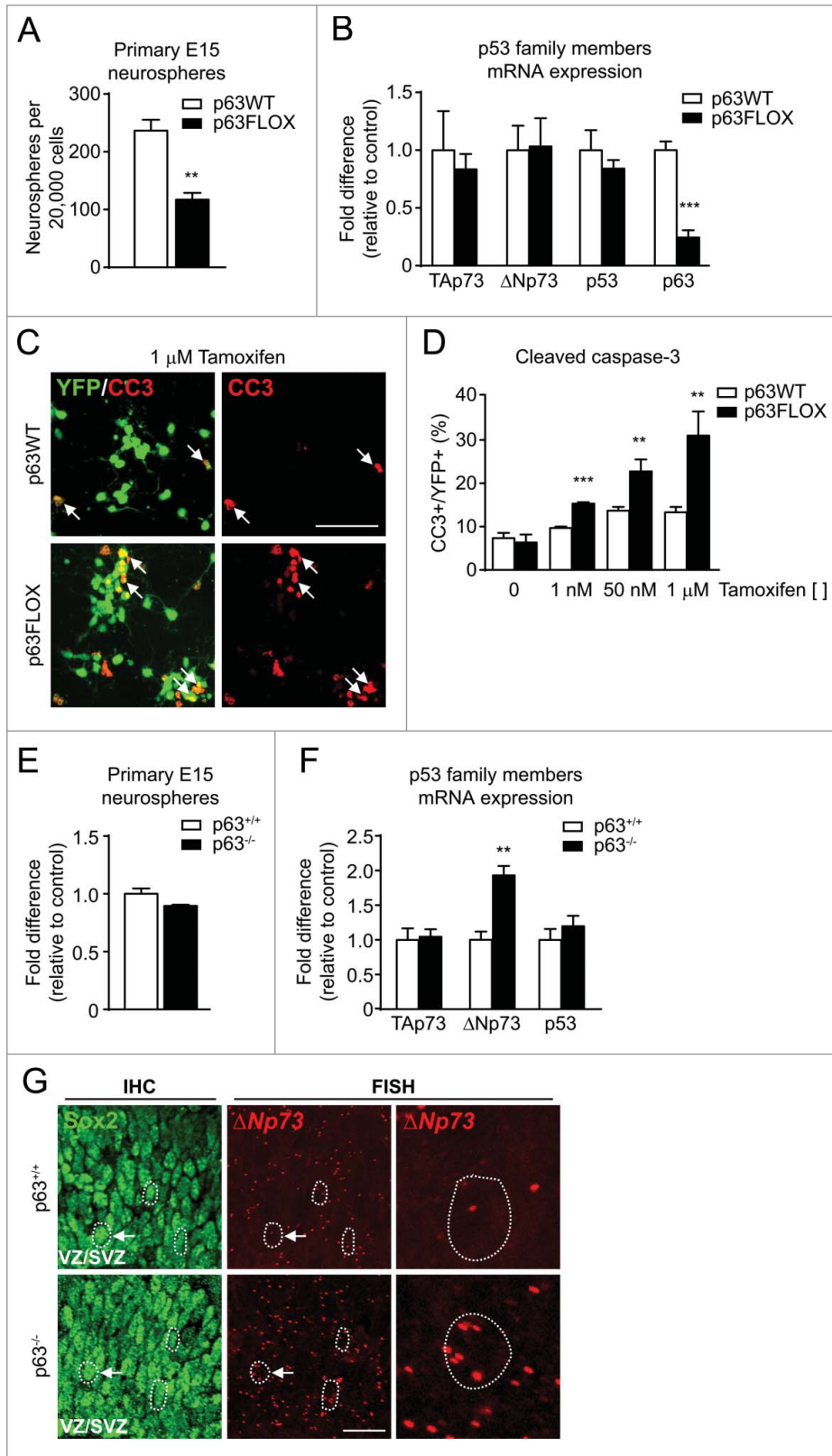


**Figure 6.** For figure legend, see page 3278.

studying p63<sup>-/-</sup> embryos, where no CNS phenotype was observed.<sup>36</sup> We show here that the lack of a phenotype when p63 is constitutively ablated is likely due to upregulation of the related prosurvival protein, ΔNp73, in neural precursors.

We previously showed that when p63 was haploinsufficient or was inducibly ablated in adult neural precursor cells (NPCs), there was apoptosis of forebrain and hippocampal NPCs, reduced adult neurogenesis, and deficits in hippocampus-dependent memory formation.<sup>36</sup> These findings, together with the current work, indicate that p63 promotes NPC survival throughout murine life. We propose that it is the ΔNp63 isoform that promotes NPC survival, since the death of embryonic cortical precursors caused by p63 knockdown was rescued by ectopic expression of ΔNp63 but not TAp63,<sup>37</sup> and since inducible knockout of ΔNp63 but not of TAp63 caused death of adult forebrain NPCs cultured as neurospheres.<sup>36</sup> How then does ΔNp63 promote survival of cortical precursor cells during embryogenesis? Our previous work indicates that it does so by antagonizing the pro-apoptotic actions of p53. In particular, when p63 was acutely knocked-down in cortical precursors, this caused increased apoptosis (as seen here with acute genetic ablation), and this cell death was rescued both in culture and *in vivo* by coincidentally knocking down p53.<sup>37</sup> This prosurvival mechanism appears to persist throughout life in neural precursors, since coincident p53 knockout completely rescued the deficits in adult NPCs and adult neurogenesis that occur in p63<sup>+/-</sup> mice.<sup>36</sup> Thus, the ΔNp63 isoform acts to promote NPC survival by antagonizing p53 and potentially other full-length family members. In this regard, ectopic expression of TAp63 induces the death of both NPCs and neurons,<sup>35,37</sup> indicating that in the nervous system, TAp63 promotes and ΔNp63 inhibits cell death.

These findings demonstrate that ΔNp63 and ΔNp73 are both key prosurvival proteins in the mammalian CNS, with ΔNp73 important for neuronal survival,<sup>19,23,37,43-45</sup> and ΔNp63



important for both NPC and newborn neuron survival.<sup>31,36,37</sup> This difference is exemplified by the finding that knockdown of  $\Delta Np73$  in the embryonic cortex caused the death of newborn neurons but not precursors,<sup>37</sup> while a similar knockdown of p63 caused the death of cortical precursors.<sup>37</sup> Thus, under normal circumstances,  $\Delta Np63$  is the most important family member with regard to NPC survival. However, our data showing upregulation of  $\Delta Np73$  expression in cortical NPCs of p63<sup>-/-</sup> mice argue that when p63 is constitutively ablated,  $\Delta Np73$  can replace the pro-survival function of  $\Delta Np63$ , thereby explaining the lack of an apparent embryonic NPC phenotype in the p63<sup>-/-</sup> mice. In normal circumstances, p73 promotes 2 other important roles in NPCs. Firstly, TAp73 enhances NPC self-renewal,<sup>26,27</sup> at least in part by suppressing neurogenic transcription by upregulating the inhibitory bHLH Hey2.<sup>26</sup> Secondly, p73 regulates the balance of p53-mediated senescence vs. apoptosis of NPCs. In particular, coincident haploinsufficiency for p73 inhibited the enhanced apoptosis of p63<sup>+/-</sup> adult NPCs, causing them instead to senesce.<sup>31</sup> Thus, it is the interplay between p63, p73 and p53 that ultimately determines NPC numbers by regulating their survival, self-renewal, and senescence.

## Materials and Methods

### Animals and tamoxifen treatment

This study was approved by the Hospital for Sick Children Animal Care Committee, in accordance with Canadian Council on Animal Care guidelines. p63<sup>+/-</sup> mice<sup>4</sup> were maintained on a C57BL/6 background as described.<sup>36</sup> p63<sup>fl/fl</sup> mice<sup>46</sup> were crossed with R26YFP<sup>fl/fl</sup> reporter mice<sup>47</sup> and nestin-CreERT2<sup>+/-</sup> mice<sup>39</sup> and then maintained through homozygous breeding pairs on a C57BL/6 background, as we have previously described.<sup>36</sup> For neuroanatomical analyses, adult pregnant female p63<sup>fl/fl</sup>; R26YFP<sup>fl/fl</sup>; nestin-CreERT2<sup>+/-</sup> and p63<sup>wt/wt</sup>; R26YFP<sup>fl/fl</sup>; nestin-CreERT2<sup>+/-</sup> mice were injected intraperitoneally once with

tamoxifen (180 mg/kg in sunflower seed oil) at gestational day 12. Mice had free access to rodent chow and water in a 12 hour dark-light cycle room.

### Immunocytochemistry and histological analysis

For morphometric analysis, immunostaining of tissue sections was performed as described.<sup>36,48</sup> Briefly, brain sections were washed with TBS buffer, permeabilized with TBS, 0.3% Triton X-100 solution, and then incubated in TBS, 5% BSA, 0.3% Triton X-100 for 1 hour as a blocking solution. Brain slices were incubated with primary antibodies in blocking solution at 4°C overnight. After TBS washes, the sections were incubated with secondary antibodies in blocking solution for 1 hour at room temperature. Finally, after TBS washes, sections were mounted in Permount solution (Thermo). In most cases, sections were counterstained with Hoechst 33258 (Sigma). TUNEL staining (Millipore) was performed according to manufacturer's instructions. Digital image acquisition was performed with Zen software (Carl Zeiss) on a Zeiss Axio Imager M2 microscope with a Hamamatsu Orca-Flash 4.0 CCD video camera. For quantification of embryonic cortical thickness, rostral, medial and caudal cortical sections were measured at 3 different points (dorsal, lateral and ventral), analyzing at least 3 similar sections/embryo from 3 different animals per genotype (for a total of at least 9 sections per genotype) using ImageJ software (NIH). For quantification of the embryonic ventricle area, a line was drawn around the perimeter of the ventricle at rostral, medial and caudal levels from at least 3 similar sections/embryo from 3 different animals per genotype. The area was calculated and values express as arbitrary units (AU) using ImageJ software. For quantification of the number of apoptotic cells, or of precursor cells and neurons, serial coronal 18  $\mu$ m sections were collected spanning the rostro-caudal extent of the E15 embryonic cortex and these were sampled and immunostained or TUNEL-stained (as relevant). For quantification of precursor and neuron numbers, we analyzed sections at the medial-lateral level, counting all marker-positive

**Figure 6 (See previous page).** (A, B) Acute ablation of p63 depletes cortical precursors but does not deregulate expression of other p53 family members. (A) p63<sup>wt/wt</sup>; R26YFP<sup>fl/fl</sup>; nestin-CreERT2<sup>+/-</sup> (p63WT) or p63<sup>fl/fl</sup>; R26YFP<sup>fl/fl</sup>; nestin-CreERT2<sup>+/-</sup> (p63FLOX) embryos were exposed to tamoxifen at E12, at E15 cortical cells were cultured under clonal neurosphere conditions, and the number of neurosphere-initiating cells was quantified. \*\*p < 0.01; n = 4 animals per genotype. (B) Quantitative RT-PCR for TAp73 mRNA,  $\Delta Np73$  mRNA, p53 mRNA and p63 mRNA in cortical neurospheres isolated from p63WT and p63FLOX as in (A). The data are expressed as fold difference relative to their corresponding control group (p63WT). \*\*\*p < 0.001; n = 4 animals per genotype. (C, D) Acute ablation of p63 induces cell death in cultured cortical precursors. (C) Representative images of primary adherent E12.5 cortical precursors cultured from p63<sup>wt/wt</sup>; R26YFP<sup>fl/fl</sup>; nestin-CreERT2<sup>+/-</sup> (p63WT, top panels) or p63<sup>fl/fl</sup>; R26YFP<sup>fl/fl</sup>; nestin-CreERT2<sup>+/-</sup> (p63FLOX, bottom panels) embryos, treated with 1  $\mu$ M tamoxifen at 2 days, and then immunostained 24 hours later for YFP (green) and cleaved caspase-3 (CC3, red). Left panel shows the merge and arrows denote cells positive for both YFP and CC3. Scale bar = 50  $\mu$ m. (D) Quantification of the proportion of YFP-positive cells that expressed CC3 in experiments as in (C), following exposure to 1 nM, 50 nM, or 1  $\mu$ M tamoxifen. The control, 0 tamoxifen cultures were treated with vehicle alone and since none of these cells expressed YFP, the proportion of total CC3-positive cells was determined. \*\*p < 0.01; \*\*\*p < 0.001; n = 3 animals per genotype. (E, F) Constitutive loss of p63 causes compensatory upregulation of  $\Delta Np73$  expression in embryonic cortical precursors. (E) E15 cortical cells were isolated from p63<sup>-/-</sup> or p63<sup>+/-</sup> embryos, were cultured under clonal neurosphere conditions, and the number of neurosphere-initiating cells was quantified. The data are expressed as fold difference relative to their corresponding control group (p63<sup>+/-</sup>). n = 6 and 5 animals for p63<sup>+/-</sup> and p63<sup>-/-</sup>, respectively. (F) Quantitative RT-PCR for TAp73 mRNA,  $\Delta Np73$  mRNA, and p53 mRNA in neurospheres isolated from p63<sup>-/-</sup> and p63<sup>+/-</sup> cortical neurospheres prepared as in (E). The data are expressed as fold difference relative to their corresponding control group (p63<sup>+/-</sup>). \*\*p < 0.01; n = 4 and 5 p63<sup>-/-</sup> and p63<sup>+/-</sup> animals, respectively. In all panels, error bars denote SEM. (G) Representative images of coronal cortical sections from E15 p63<sup>+/-</sup> and p63<sup>-/-</sup> embryos, immunostained for the pan-precursor marker Sox2 (green, left panels) and hybridized for  $\Delta Np73$  mRNA (red, right panels, same fields of view). The white lines and arrows delineate Sox2-positive precursors that contain  $\Delta Np73$  mRNA-positive foci. The ventricular/subventricular zones (VZ/SVZ) are indicated. IHC = immunohistochemistry. FISH = fluorescent *in situ* hybridization. Scale bar = 50  $\mu$ m. See text for the quantification of the data of Fig. 6G.

cells in a 200  $\mu\text{m}$  wide strip of the cortex extending from the meninges to the ventricle. For cell death analysis, every TUNEL or cleaved caspase-3 positive cell was counted on sections at rostral, medial and caudal levels. In all cases, we analyzed at least 3 similar cortical sections/embryo from 3 different embryos per genotype (for a total of at least 9 sections per genotype).

### In situ hybridization

Fluorescent *in situ* hybridization (FISH) was performed with probes targeting  $\Delta\text{Np}73$  (National Center for Biotechnology Information [NCBI] Nucleotide Reference Sequence [RefSeq] database accession number NM\_001126330.1) using the RNA-scope kit (Advanced Cell Diagnostics), according to the manufacturer's instructions. Briefly,<sup>49</sup> freshly dissected brains of E15 embryos in OCT were snap-frozen in liquid nitrogen and cryo-sectioned coronally at 18  $\mu\text{m}$ . Sections were 4% post-fixed with paraformaldehyde and washed with ethanol, followed by tissue pretreatment, probe hybridization and signal amplification. Positive hybridization was identified as punctate dots. After FISH, immunostaining was performed for Sox2. Z-stack images were taken with an optical slice thickness of 0.1  $\mu\text{m}$ , with a 40X objective on a Zeiss Axio Imager M2 microscope with an Apo-Tome device and with a Hamamatsu Orca-Flash 4.0 CCD video camera. The proportion of  $\Delta\text{Np}73$  mRNA-Sox2-double positive cells was quantified from z-stacked images from random regions of the VZ/SVZ. The number of  $\Delta\text{Np}73$  mRNA foci per Sox2-positive cell was quantified from 200–300 z-stacked images from random regions of the VZ/SVZ.

### Cortical precursor cell cultures and quantification

E12.5 cortical precursors were cultured from  $\text{p}63^{\text{wt/wt}}$ ; R26YFP <sup>$\beta/\beta$</sup> ;nestin-CreERT2 <sup>$+/O$</sup>  or  $\text{p}63^{\beta/\beta}$ ;R26YFP <sup>$\beta/\beta$</sup> ;nestin-CreERT2 <sup>$+/O$</sup>  E12.5 cortices as described previously.<sup>40,48</sup> Plating density was 125,000–150,000 cells/ml. For tamoxifen treatment *in vitro*, tamoxifen was dissolved in DMSO so that the final volume of DMSO was approximately 0.1% of the total volume of medium. In all experiments, DMSO alone was used as a vehicle control. Cells were treated with tamoxifen at day 2 in culture, and analyzed one day later. For quantification, immunostaining and image acquisition were performed as described above, and > 100 cells per condition per experiment were counted and analyzed, and experiments were performed with 3 embryos per genotype, analyzed individually.

### Antibodies

The primary antibodies used for immunostaining were chicken anti-GFP (1:1000; Abcam), rabbit anti-Pax6 (1:1000; Covance), rabbit anti-Tbr2 (1:250; Abcam), chicken anti-Tbr2 (1:400; Abcam), mouse anti-Satb2 (1:400; Abcam), mouse anti- $\beta$ III-tubulin (1:1000; Covance), rabbit anti- $\beta$ III-tubulin (1:1000; Covance), rabbit anti-cleaved caspase 3 (1:200; Millipore), rabbit anti-Sox2 (1:200; Cell Signaling Technology), and goat anti-Sox2 (1:500; Santa Cruz). The secondary antibodies used for immunostaining were Alexa Fluor 555-conjugated donkey anti-mouse and anti-rabbit IgG (1:1000; Molecular Probes), Alexa Fluor 488-conjugated donkey anti-mouse, and anti-rabbit

IgG (1:1000; Molecular Probes), Alexa Fluor 488-conjugated chicken anti-rat IgG (1:1000; Molecular Probes), and Cy3-conjugated donkey anti-goat antibody (1:1000; Jackson ImmunoResearch).

### Neurosphere cultures

To make embryonic cortical neurospheres, cortices from E15  $\text{p}63^{\text{wt/wt}}$ ; R26YFP <sup>$\beta/\beta$</sup> ;nestin-CreERT2 <sup>$+/O$</sup>  or  $\text{p}63^{\beta/\beta}$ ;R26YFP <sup>$\beta/\beta$</sup> ;nestin-CreERT2 <sup>$+/O$</sup>  embryos, previously injected with tamoxifen on E12, were mechanically triturated in serum-free medium containing 20 ng/mL EGF (Sigma), 10 ng/mL FGF2 (Sigma), and 2  $\mu\text{g}/\text{mL}$  heparin (Sigma). For quantification, cells were plated at clonal density<sup>50</sup> in 6-well dishes (2 ml/well). After 6 d in culture, primary neurospheres containing at least 50 cells were counted, and were then collected for mRNA expression analysis. A similar procedure was used to make embryonic cortical neurospheres from E15  $\text{p}63^{+/+}$  or  $\text{p}63^{-/-}$  embryos.

### Quantitative RT-PCR

RNA was isolated from primary neurospheres or dissected E15 cortices using the E.Z.N.A. Total RNA Kit I (Omega Bio-tek), and was treated with DNase I using the E.Z.N.A. RNase-Free DNase I Set (Omega Bio-tek). cDNA was synthesized from 1  $\mu\text{g}$  of total RNA using RevertAid H Minus M-MuLV Reverse Transcriptase (Fermentas), and quantitative PCR was performed using Lightcycler 480 SYBR Green I Master mix (Roche), following the manufacturer's instructions. The following primers were used for quantitative PCR: TAp73F – GCACCTACTTTGACCTCCCC, TAp73R – GCACTGCTGAGCAAATTGAAC,  $\Delta\text{Np}73\text{F}$  – CTA CCCCTACCCACCTAG,  $\Delta\text{Np}73\text{R}$  – CTGAGCAAATTGA ACTGGGC, pan-p63F – CGGAAGGCAGATGAAGACAG, pan-p63R – GGGATCTCCGTTTCTTGATGG, p53F – CTCT CCCCCGAAAAGAAAAA, p53R – CGGAACATCTCGA AGCGTTTA, PUMAF – GTGACCACTGGCATTTCATTTG, PUMAR – CTCCTCCCTCTTCTGAGACTT, GAPDHF – GG GTGTGAACCACGAGAAATA, GAPDHR – CTGTGGTCATGAGCCCTTC. GAPDH mRNA was used as an endogenous control for all reactions, and all reactions were performed in triplicate. Quantitative PCRs were run on a C1000 Touch Thermal Cycler (Bio-Rad), and analyzed using Bio-Rad CFX Manager Software (Bio-Rad).

### Statistical analysis

Statistics were performed using 2-tailed Student's *t*-test unless otherwise indicated in the text. To analyze the multi-group neuroanatomical studies, we used one-way ANOVA unless otherwise indicated in the text. Significant interactions or main effects were further analyzed using Newman-Keuls post-hoc tests. All tests were performed using Prism 5 (GraphPad). In all cases, error bars indicate standard error of the mean.

### Disclosure of Potential Conflicts of Interest

No potential conflicts of interest were disclosed.

## Acknowledgments

We thank Alea Mills (Cold Spring Harbor Laboratory) for the generous gift of the p63<sup>-/-</sup> and p63<sup>fl/fl</sup> mice. We thank Benigno Aquino and Adelaida Kolaj for technical assistance.

## Funding

This work was funded by CIHR grants MOP-38021 and MOP-14446 to F.D.M. and D.R.K. G.I.C. was funded by fellowships from the Heart and Stroke Foundation of Canada and

Becas Chile, F.D.M. and D.R.K. hold Canada Research Chairs, and F.D.M. is an HHMI Senior International Research Scholar.

## Author Contributions

G.I.C. carried out most of the experiments and co-wrote the paper. M.P.F. carried out mRNA expression analysis. F.D.M. and D.R.K. co-supervised all experiments and co-wrote the paper.

## References

1. Donehower LA, Harvey M, Slagle BL, McArthur MJ, Montgomery CA Jr, Butel JS, Bradley A. Mice deficient for p53 are developmentally normal but susceptible to spontaneous tumours. *Nature* 1992; 356:215-21; PMID:1552940; <http://dx.doi.org/10.1038/356215a0>
2. Jacks T, Remington L, Williams BO, Schmitt EM, Halachmi S, Bronson RT, Weinberg RA. Tumor spectrum analysis in p53-mutant mice. *Curr Biol* 1994; 4:1-7; PMID:7922305; [http://dx.doi.org/10.1016/S0960-9822\(00\)00002-6](http://dx.doi.org/10.1016/S0960-9822(00)00002-6)
3. Sah VP, Attardi LD, Mulligan GJ, Williams BO, Bronson RT, Jacks T. A subset of p53-deficient embryos exhibit exencephaly. *Nat Genet* 1995; 10:175-80; PMID:7663512; <http://dx.doi.org/10.1038/ng0695-175>
4. Mills AA, Zheng B, Wang XJ, Vogel H, Roop DR, Bradley A. p63 is a p53 homologue required for limb and epidermal morphogenesis. *Nature* 1999; 398:708-13; PMID:10227293; <http://dx.doi.org/10.1038/19531>
5. Yang A, Schweitzer R, Sun D, Kaghad M, Walker N, Bronson RT, Tabin C, Sharpe A, Caput D, Crum C, et al. p63 is essential for regenerative proliferation in limb, craniofacial and epithelial development. *Nature* 1999; 398:714-8; PMID:10227294; <http://dx.doi.org/10.1038/19539>
6. Yang A, Walker N, Bronson R, Kaghad M, Oosterwegel M, Bonnin J, Vagner C, Bonnet H, Dikkes P, Sharpe A, et al. p73-deficient mice have neurological, pheromonal and inflammatory defects but lack spontaneous tumours. *Nature* 2000; 404:99-103; PMID:10716451; <http://dx.doi.org/10.1038/35003607>
7. Su X, Paris M, Gi YJ, Tsai KY, Cho MS, Lin YL, Bier-naskie JA, Sinha S, Prives C, Pevny LH, et al. TAp63 prevents premature aging by promoting adult stem cell maintenance. *Cell Stem Cell* 2009; 5:64-75; PMID:19570515; <http://dx.doi.org/10.1016/j.stem.2009.04.003>
8. Fletcher RB, Prasol MS, Estrada J, Baudhuin A, Vranizan K, Choi YG, Ngai J. p63 regulates olfactory stem cell self-renewal and differentiation. *Neuron* 2011; 72:748-59; PMID:22153372; <http://dx.doi.org/10.1016/j.neuron.2011.09.009>
9. Oh JE, Kim RH, Shin KH, Park NH, Kang MK. DeltaNp63 $\alpha$  protein triggers epithelial-mesenchymal transition and confers stem cell properties in normal human keratinocytes. *J Biol Chem* 2011; 286:38757-67; PMID:21880709; <http://dx.doi.org/10.1074/jbc.M111.244939>
10. Rouleau M, Medawar A, Hamon L, Shvitiel S, Wolchinsky Z, Zhou H, De Rosa L, Candi E, de la Forest Divonne S, Mikkola ML, et al. TAp63 is important for cardiac differentiation of embryonic stem cells and heart development. *Stem Cells* 2011; 29:1672-83; PMID:21898690; <http://dx.doi.org/10.1002/stem.723>
11. Feron G, Thomason HA, Antonini D, De Rosa L, Hu B, Gemei M, Zhou H, Ambrosio R, Rice DP, Acampora D, et al. Mutant p63 causes defective expansion of ectodermal progenitor cells and impaired FGF signalling in AEC syndrome. *EMBO Mol Med* 2012; 4:192-205; PMID:22247000; <http://dx.doi.org/10.1002/emmm.201100199>
12. Pignon JC, Grisanzio C, Geng Y, Song J, Shivdasani RA, Signoretti S. p63-expressing cells are the stem cells of developing prostate, bladder, and colorectal epithelia. *Proc Natl Acad Sci U S A* 2013; 110:8105-10; PMID:23620512; <http://dx.doi.org/10.1073/pnas.1221216110>
13. Forster N, Saladi SV, van Braagt M, Sfondouris ME, Jones FE, Li Z, Ellisen LW. Basal cell signaling by p63 controls luminal progenitor function and lactation via NRG1. *Dev Cell* 2014; 28:147-60; PMID:24412575; <http://dx.doi.org/10.1016/j.devcel.2013.11.019>
14. Inoue S, Tomasini R, Rufini A, Elia AJ, Agostini M, Amelio I, Cescon D, Dinsdale D, Zhou L, Harris IS, et al. p73 is required for spermatogenesis and the maintenance of male fertility. *Proc Natl Acad Sci U S A* 2014; 111:1843-8; PMID:24449892; <http://dx.doi.org/10.1073/pnas.1323416111>
15. Fernandez-Alonso R, Martin-Lopez M, Gonzalez-Cano L, Garcia S, Castrillo F, Diez-Prieto I, Fernandez-Corona A, Lorenzo-Marcos ME, Li X, Claesson-Welsh L, et al. p73 is required for endothelial cell differentiation, migration and the formation of vascular networks regulating VEGF and TGF $\beta$  signaling. *Cell Death Differ* 2015; 22(8):1287-99; PMID:25571973
16. Ouyang H, Xue Y, Lin Y, Zhang X, Xi L, Patel S, Cai H, Luo J, Zhang M, Zhang M, et al. WNT7A and PAX6 define corneal epithelium homeostasis and pathogenesis. *Nature* 2014; 511:358-61; PMID:25030175; <http://dx.doi.org/10.1038/nature13465>
17. Memmi EM, Sanarico AG, Giacobbe A, Peschiaroli A, Frezza V, Cicalese A, Pisati F, Tosoni D, Zhou H, Tonon G, et al. p63 sustains self-renewal of mammary cancer stem cells through regulation of Sonic Hedgehog signaling. *Proc Natl Acad Sci U S A* 2015; 112:3499-504; PMID:25739959; <http://dx.doi.org/10.1073/pnas.1500762112>
18. Yang A, McKeon F. P63 and P73: P53 mimics, menaces and more. *Nat Rev Mol Cell Biol* 2000; 1:199-207; PMID:11252895; <http://dx.doi.org/10.1038/35043127>
19. Wilhelm MT, Rufini A, Wetzel MK, Tsuchihara K, Inoue S, Tomasini R, Irie-Youten A, Wakeham A, Arsenian-Henriksson M, Melino G, et al. Isoform-specific p73 knockout mice reveal a novel role for delta Np73 in the DNA damage response pathway. *Genes Dev* 2010; 24:549-60; PMID:20194434; <http://dx.doi.org/10.1101/gad.1873910>
20. Pozniak CD, Radinovic S, Yang A, McKeon F, Kaplan DR, Miller FD. An anti-apoptotic role for the p53 family member, p73, during developmental neuron death. *Science* 2000; 289:304-6; PMID:10894779; <http://dx.doi.org/10.1126/science.289.5477.304>
21. Lee AF, Ho DK, Zanassi P, Walsh GS, Kaplan DR, Miller FD. Evidence that DeltaNp73 promotes neuronal survival by p53-dependent and p53-independent mechanisms. *J Neurosci* 2004; 24:9174-84; PMID:15483136; <http://dx.doi.org/10.1523/JNEUROSCI.1588-04.2004>
22. Walsh GS, Orike N, Kaplan DR, Miller FD. The invulnerability of adult neurons: a critical role for p73. *J Neurosci* 2004; 24:9638-47; PMID:15509751; <http://dx.doi.org/10.1523/JNEUROSCI.1299-04.2004>
23. Pozniak CD, Barnabé-Heider F, Rymar VV, Lee AF, Sadikot AF, Miller FD. p73 is required for survival and maintenance of CNS neurons. *J Neurosci* 2002; 22:9800-9; PMID:12427836
24. Tomasini R, Tsuchihara K, Wilhelm M, Fujitani M, Rufini A, Cheung CC, Khan F, Irie-Youten A, Wakeham A, Tsao MS, et al. TAp73 knockout shows genomic instability with infertility and tumor suppressor functions. *Genes Dev* 2008; 22:2677-91; PMID:18805989; <http://dx.doi.org/10.1101/gad.1695308>
25. Agostini M, Tucci P, Chen H, Knight RA, Bano D, Nicotera P, McKeon F, Melino G. p73 regulates maintenance of neural stem cell. *Biochem Biophys Res Commun* 2010; 403:13-7; PMID:20977890; <http://dx.doi.org/10.1016/j.bbrc.2010.10.087>
26. Fujitani M, Cancino GI, Dugani CB, Weaver IC, Gauthier-Fisher A, Paquin A, Mak TW, Wojtowicz MJ, Miller FD, Kaplan DR. TAp73 acts via the bHLH Hey2 to promote long-term maintenance of neural precursors. *Curr Biol* 2010; 20:2058-65; PMID:21074438; <http://dx.doi.org/10.1016/j.cub.2010.10.029>
27. Gonzalez-Cano L, Herreros-Villanueva M, Fernandez-Alonso R, Ayuso-Sacido A, Meyer G, Garcia-Verdugo JM, Silva A, Marques MM, Marin MC. p73 deficiency results in impaired self renewal and premature neuronal differentiation of mouse neural progenitors independently of p53. *Cell Death Dis.* 2010; 1: e109; PMID:21368881; <http://dx.doi.org/10.1038/cddis.2010.87>
28. Talos F, Abraham A, Vaseva AV, Holemowski L, Tsrirka SE, Scheel A, Bode D, Dobbstein M, Brück W, Moll UM. p73 is an essential regulator of neural stem cell maintenance in embryonal and adult CNS neurogenesis. *Cell Death Differ* 2010; 17:1816-29; PMID:21076477; <http://dx.doi.org/10.1038/cdd.2010.131>
29. Agostini M, Tucci P, Killick R, Candi E, Sayan BS, Rivetti di Val Cervo P, Nicotera P, McKeon F, Knight RA, Mak TW, Melino G. Neuronal differentiation by TAp73 is mediated by microRNA-34a regulation of synaptic protein targets. *Proc Natl Acad Sci U S A* 2011; 108:21093-8; PMID:22160687; <http://dx.doi.org/10.1073/pnas.1112061109>
30. Niklison-Chirou MV, Steinert JR, Agostini M, Knight RA, Dinsdale D, Cattaneo A, Mak TW, Melino G. TAp73 knockout mice show morphological and functional nervous system defects associated with loss of p75 neurotrophin receptor. *Proc Natl Acad Sci U S A* 2013; 110:18952-7; PMID:24190996; <http://dx.doi.org/10.1073/pnas.1221172110>
31. Fatt MP, Cancino GI, Miller FD, Kaplan DR. p63 and p73 coordinate p53 function to determine the balance between survival, cell death, and senescence in adult neural precursor cells. *Cell Death Differ* 2014; 21:1546-59; PMID:24809925; <http://dx.doi.org/10.1038/cdd.2014.61>
32. Cancino GI, Toledo EM, Leal NR, Hernandez DE, Yévenes LF, Inestrosa NC, Alvarez AR. STI571 prevents apoptosis, tau phosphorylation and behavioural impairments induced by Alzheimer's beta-amyloid deposits. *Brain* 2008; 131:2425-42; PMID:18559370; <http://dx.doi.org/10.1093/brain/awn125>

33. Wetzel MK, Naska S, Laliberté CL, Rymer VV, Fujitani M, Biernaskie JA, Cole CJ, Lerch JP, Spring S, Wang SH, et al. p73 regulates neurodegeneration and phospho-tau accumulation during aging and Alzheimer's disease. *Neuron* 2008; 59:708-21; PMID:18786355; <http://dx.doi.org/10.1016/j.neuron.2008.07.021>
34. Cancino GI, Miller FD, Kaplan DR. p73 haploinsufficiency causes tau hyperphosphorylation and tau kinase dysregulation in mouse models of aging and Alzheimer's disease. *Neurobiol Aging* 2013; 34:387-99; PMID:22592019; <http://dx.doi.org/10.1016/j.neurobiolaging.2012.04.010>
35. Jacobs WB, Govoni G, Ho D, Atwal JK, Barnabe-Heider F, Keyes WM, Mills AA, Miller FD, Kaplan DR. p63 is an essential proapoptotic protein during neural development. *Neuron* 2005; 48:743-56; PMID:16337913; <http://dx.doi.org/10.1016/j.neuron.2005.10.027>
36. Cancino GI, Yiu AP, Fatt MP, Dugani CB, Flores ER, Frankland PW, Josselyn SA, Miller FD, Kaplan DR. p63 Regulates adult neural precursor and newly born neuron survival to control hippocampal-dependent Behavior. *J Neurosci* 2013; 33:12569-85; PMID:23904595; <http://dx.doi.org/10.1523/JNEUROSCI.1251-13.2013>
37. Dugani CB, Paquin A, Fujitani M, Kaplan DR, Miller FD. p63 antagonizes p53 to promote the survival of embryonic neural precursor cells. *J Neurosci* 2009; 29:6710-21; PMID:19458240; <http://dx.doi.org/10.1523/JNEUROSCI.5878-08.2009>
38. Holembowski L, Schulz R, Talos F, Scheel A, Wolff S, Dobbstein M, Moll U. While p73 is essential, p63 is completely dispensable for the development of the central nervous system. *Cell Cycle* 2011; 10:680-9; PMID:21293190; <http://dx.doi.org/10.4161/cc.10.4.14859>
39. Imayoshi I, Sakamoto M, Ohtsuka T, Takao K, Miyakawa T, Yamaguchi M, Mori K, Ikeda T, Ito-hara S, Kageyama R. Roles of continuous neurogenesis in the structural and functional integrity of the adult forebrain. *Nat Neurosci.* 2008; 11:1153-61; PMID:18758458; <http://dx.doi.org/10.1038/nn.2185>
40. Zander MA, Burns SE, Yang G, Kaplan DR, Miller FD. Snail coordinately regulates downstream pathways to control multiple aspects of mammalian neural precursor development. *J Neurosci* 2014; 34:5164-75; PMID:24719096; <http://dx.doi.org/10.1523/JNEUROSCI.0370-14.2014>
41. Tsui D, Vessey JP, Tomita H, Kaplan DR, Miller FD. FoxP2 regulates neurogenesis during embryonic cortical development. *J Neurosci* 2013; 33:244-58; PMID:23283338; <http://dx.doi.org/10.1523/JNEUROSCI.1665-12.2013>
42. Ory B, Ellisen LW. A microRNA-dependent circuit controlling p63/p73 homeostasis: p53 family crosstalk meets therapeutic opportunity. *Oncotarget.* 2011; 2:259-64; PMID:21436470
43. Abraham H, Pérez-García CG, Meyer G. p73 and Reelin in Cajal-Retzius cells of the developing human hippocampal formation. *Cereb Cortex* 2004; 14:484-95; PMID:15054064; <http://dx.doi.org/10.1093/cercor/bhh010>
44. Meyer G, Cabrera Socorro A, Perez Garcia CG, Martinez Millan L, Walker N, Caput D. Developmental roles of p73 in Cajal-Retzius cells and cortical patterning. *J Neurosci* 2004; 24:9878-87; PMID:15525772; <http://dx.doi.org/10.1523/JNEUROSCI.3060-04.2004>
45. Tissir F, Ravni A, Achouri Y, Riethmacher D, Meyer G, Goffinet AM. DeltaNp73 regulates neuronal survival in vivo. *Proc Natl Acad Sci USA* 2009; 106:16871-6; PMID:19805388; <http://dx.doi.org/10.1073/pnas.0903191106>
46. Mills AA, Qi Y, Bradley A. Conditional inactivation of p63 by Cre-mediated excision. *Genesis* 2002; 32:138-41; PMID:11857801; <http://dx.doi.org/10.1002/gene.10067>
47. Lagace DC, Whitman MC, Noonan MA, Ables JL, DeCarolis NA, Arguello AA, Donovan MH, Fischer SJ, Farnbaum LA, Beech RD, et al. Dynamic contribution of nestin-expressing stem cells to adult neurogenesis. *J Neurosci* 2007; 27:12623-9; PMID:18003841; <http://dx.doi.org/10.1523/JNEUROSCI.3812-07.2007>
48. Gallagher D, Voronova A, Zander MA, Cancino GI, Bramall A, Krause MP, Abad C, Tekin M, Neilsen PM, Callen DF, et al. Ankrd11 is a chromatin regulator involved in autism that is essential for neural development. *Dev Cell* 2015; 32:31-42; PMID:25556659; <http://dx.doi.org/10.1016/j.devcel.2014.11.031>
49. Yang G, Smibert CA, Kaplan DR, Miller FD. An eIF4E1/4E-T complex determines the genesis of neurons from precursors by translationally repressing a proneurogenic transcription program. *Neuron* 2014; 84:723-39; PMID:25456498; <http://dx.doi.org/10.1016/j.neuron.2014.10.022>
50. Coles-Takabe BL, Brain I, Purpura KA, Karpowicz P, Zandstra PW, Morshead CM, van der Kooy D. Don't look: growing clonal versus nonclonal neural stem cell colonies. *Stem Cells* 2008; 26:2938-44; PMID:18757294; <http://dx.doi.org/10.1634/stemcells.2008-0558>